

Constructal theory of particle agglomeration and design of air-cleaning devices

A H Reis^{1,2}, A F Miguel^{1,2} and A Bejan³

¹ Geophysics Centre of Évora, Rua Romão Ramalho 59, 7000-671 Évora, Portugal

² Department of Physics, University of Évora, Apartado 94, 7002-554 Évora, Portugal

³ Department of Mechanical Engineering and Materials Science, Duke University, Durham, NC 27708-0300, USA

E-mail: ahr@uevora.pt

Received 2 February 2006, in final form 27 March 2006

Published 5 May 2006

Online at stacks.iop.org/JPhysD/39/2311

Abstract

In this paper we propose a constructal approach to understanding and predicting the morphology of agglomerates of aerosol particles and also to the design of air-cleaning devices. We show that particle agglomeration begins in spherical shape and switches to needle-shaped agglomeration, which performs best as a particle collector at long times. The shape of the needle depends on the dipolar moment of the particles, while the critical number of particles prior to switching to needle shape does not depend on the particle properties. We also show how constructal theory leads to the design of air-cleaning devices that achieve maximum performance per unit volume, under the imposed global constraints. The optimal geometry (internal spacing) of devices composed of parallel-plate channels or tubes and porous filters is shown to depend on known non-dimensional numbers that characterize particle deposition. The work reported in this paper adds to many studies that show how constructal theory provides a deterministic basis for the generation of flow configuration everywhere.

Nomenclature

a	spacing between charges (dipole), m	\dot{N}	current of particles, s^{-1}
A	area, m^2	p	pressure, Pa
B	pressure drop number	P_0	Poiseuille number
c_c	Cunningham factor	q	charge, C
C	concentration, $kg\ m^{-3}$	Re	Reynolds number
d	diameter of cylinder or distance, m	Sc	Schmidt number
\dot{d}	speed of diameter growth, $m\ s^{-1}$	Sh	Sherwood number
D	diameter of sphere, m	t	time, s
D_{df}	diffusion coefficient, $m^2\ s^{-1}$	U	velocity, $m\ s^{-1}$
D_h	hydraulic diameter, m	V	volume, m^3
F	force, N	H, L, W	height, length, width, m
H	height, m	Z	wetted perimeter, m
K	constant (equation (11)), $m^{5/2}\ s^{-2}$	<i>Greek symbols</i>	
L	length, m	α, φ, θ	angle, rad
\dot{L}	speed of needle tip growth, $m\ s^{-1}$	ε	porosity
m	particle transfer density, $kg\ m^{-3}\ s^{-1}$	ε_0	electric permittivity, $C^2\ N^{-1}\ m^{-2}$
\dot{n}	flux of particles, $s^{-1}\ m^{-2}$	ϕ	number of tubes/plates
		η	viscosity, $N\ s\ m^{-2}$

κ	permeability, m^2
λ	particle transfer coefficient, m s^{-1}
μ	dipole moment, C m
ρ	air density, kg m^{-3}
σ	surface density of charge, C m^{-2}
τ	shear stress, N m^{-2}

Subscripts

C	charge/dipole
cy	cylinder
D	drag
op	optimized
p	particle
pl	plane
sp	sphere

1. Introduction

Aerosol particles originate naturally (e.g. dust, salt, pollen, microbes, viruses, etc) and as a result of industrial activity, incineration and combustion processes. Numerous epidemiological and toxicological studies have linked ambient particulate matter, especially submicrometre particles, with adverse health effects. Aerosol particles are also potentially hazardous for electronic equipment and works of fine art.

Filtration is a process used extensively for removing suspended particulate matter from gas streams. Even though this is a long established practice, the majority of the technologies available for filtering aerosol particles capture only a small fraction of submicrometre particles [1, 2]. The development of filtering devices that can collect aerosol particles efficiently is therefore a key issue. While much attention has been focused on predicting the rate of deposition/agglomeration of particles, only recently experimental and simulation studies have been devoted to the morphology of the deposits. Knowledge of the evolution of deposit morphology is important in nano-material processing [3, 4] and fundamental to the progress of modelling filtration process [2] and the performance of such devices [5].

The objective of this paper is to bring to the attention of aerosol research a new physics principle—the constructal law [6, 7]—the implications of which are general and important in natural, industrial and biological systems [7, 8]. Constructal theory is about the phenomenon of generation of architecture in flow systems. The acquisition of geometry is the mechanism by which the system meets its global objectives under the existing constraints. The objective is the maximization of global access for all the currents that flow through the system. Flow resistances cannot be eliminated. They can be balanced against each other, so that their global effect is minimized. This evolutionary process of balancing and distributing resistances constitutes the generation of flow configuration. The resulting (constructal) configuration is deduced from principle, not assumed, and not postulated.

The global maximization of flow access predicts in a simple manner not only the evolution of man-made systems but also the shapes and structures that occur in nature. The rapid development of constructal theory was reviewed by several authors [7–11].

In this paper we use constructal theory to describe the morphology of agglomerates of particles. In addition,

we propose a methodology to build optimized air-cleaning devices. Two filter designs are optimized based on the method of intersection of asymptotes, such that the capture of particles is maximized per unit of used volume: (i) devices composed of parallel-plate channels or parallel tubes and (ii) porous filter structures. The filter architectures developed in this paper should be of interest in both aerosol science and manufacturing of filters.

2. Shape and structure of agglomerates of particles

Agglomeration is the process by which particles collide to form larger particles, which typically have greater settling speed. Deposition describes the process by which particles collide and attach to surfaces. Collisions and the coming together of multiple particles result in aggregates that usually have dendritic shape. This pattern of agglomeration and deposition has a profound effect on filtration process [12, 13], nano-materials' processing [3, 4] and the performance of such devices [5].

Agglomerates of aerosol particles often have dendritic shapes that can be observed experimentally [13] or based on numerical simulations [14–17]. Is dendritic shape the prevalent and natural form of particle agglomeration? If so, why do aggregates of particles exhibit this particular shape?

Here we address these issues in the framework provided by constructal theory [6]. The *constructal law requires the architecture of the aggregate of particles to evolve in time in such a way that the global rate of accumulation of the particles is maximized*. The generation of optimized architectures should bring the entire flow system (ambient + particles) to equilibrium in the fastest way possible.

Consider the following illustration of why the occurrence of dendritic agglomerates can be anticipated by the constructal law. The forces that make aerosol particles stick onto collectors (filter/beds/previously deposited particles) are of the electrical type. In fact, it is impossible to find electrically neutral surfaces in contact with air. Electrical bonds may occur through interactions of various types (e.g. charge–charge, charge–dipole, dipole–dipole, etc). However, charge–charge interactions cancel the existing surface charge, and only the charge–dipole interaction ensures a steady and continuing process of deposition, because a dipole–charge bond leaves the total charge amount invariant (figure 1). This is a very common form of interaction because almost all particles have significant dipolar moments.

Assume that a spherical surface with a surface charge density σ collects particles from a surrounding cloud of dipolar particles having uniform concentration C_p in stagnant air. Before binding to the surface, the small particles travel radially under the influence of charge–dipole forces. For a very small particle travelling with a Stokes flow velocity u_p , the drag force F_D is

$$F_D = \frac{3\pi\eta d_p u_p}{c_c}. \quad (1)$$

Here η is the dynamic fluid viscosity, d_p is the particle diameter and c_c is the Cunningham correction factor [8]. The charge–dipole force F_C of attraction between the surface and a particle

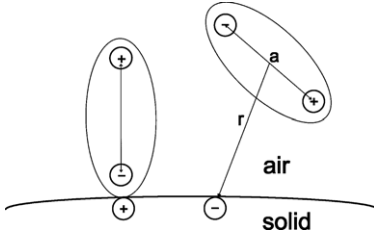


Figure 1. Dipolar particles near a charged surface.

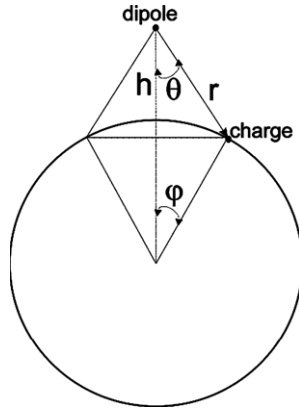


Figure 2. Interaction between dipole and a charged (spherical or cylindrical) surface.

of dipolar moment $\vec{\mu} = q\vec{a}$ is

$$F_C = \frac{1}{4\pi\epsilon_0} \frac{\int_A \mu\sigma \cos\alpha \, dA}{r^3}, \quad (2)$$

where ϵ is the electric permittivity of the air and r is the distance between the dipole centre and the surface charge (figure 2). The evaluation of F_C may be carried out for the cases of spherical, cylindrical and planar geometries in the following way.

For spherical geometry, by considering figure 2, one has the following relationships:

$$r \sin\theta = R \sin\varphi, \quad (3)$$

$$r \cos\theta + R \cos\varphi = R + h. \quad (4)$$

In order to evaluate the charge–dipole force in the vicinity of the surface we consider $h \sim a/2$, $\sin\theta \sim 1$. Half of dipolar particles is repelled from the surface while the other half is attracted to the surface. The mean value of $\cos\alpha$ is $2/\pi$. Therefore the mean attractive force between surface charges and dipole (see equation (2)) reads as

$$F_{Csp} \sim \frac{\mu\sigma}{\pi\epsilon_0 R} \int_0^{\varphi_0} \frac{d\varphi}{\sin^2\varphi}. \quad (5)$$

After evaluating the integral in (5) and with $\sin\varphi_0 \sim (h/R)^{1/2}$, $h \sim a/2$, $\mu = qa$ and $R = D/2$ one has

$$F_{Csp} \sim \frac{\sigma}{\pi\epsilon_0} (q\mu)^{1/2} D^{-1/2}. \quad (6)$$

For the cylindrical geometry with $\cos\varphi_0 \sim 1$, equation (2) reads as

$$F_{Ccy} \sim \frac{\mu\sigma}{2\pi^2\epsilon_0 R} \int_0^{\varphi_0} d\varphi \int_{-\infty}^{+\infty} \frac{d(L/R)}{(L^2/R^2 + \sin^2\varphi)^{3/2}} \quad (7)$$

or, with $d = R/2$,

$$F_{Ccy} \sim \frac{2\sigma}{\pi^2\epsilon_0} (q\mu)^{1/2} d^{-1/2}. \quad (8)$$

Finally, for the force between dipole and planar charged surface one has

$$F_{Cpl} = \frac{2\sigma\mu}{\pi\epsilon_0} \int_0^{\pi/2} \frac{\sin\theta \cos^2\theta \, d\theta}{a} \quad (9)$$

or

$$F_{Cpl} = \frac{2\sigma q}{3\pi\epsilon_0}. \quad (10)$$

We assume that both forces, F_D and F_C , cancel each other so that just before particles bind to the surface they travel with the velocity u_p . Hence, from equations (1) and (6) we may calculate the flux of particles ($\dot{n}_{sp} = C_p u_p/2$, where C_p is the concentration of dipolar particles in the vicinity of the surface) towards the surface of the sphere as

$$\dot{n}_{sp} = \frac{K}{v_p} D^{-1/2}, \quad (11)$$

where

$$K = \frac{C_p \sigma c_c v_p}{6\pi^2 \epsilon_0 \eta d_p} (q\mu)^{1/2} \quad (11a)$$

and v_p is the particle volume.

By using equations (1) and (8), for a cylindrical surface of diameter d we calculate the flux of particles ($\dot{n}_{cy} = C_p u_p/2$) towards the surface as

$$\dot{n}_{cy} = \frac{2K}{\pi v_p} d^{-1/2}, \quad (12)$$

while with the help of equations (1) and (10) the flow of particles towards a planar charged surface reads as

$$\dot{n}_{pl} = \frac{2K}{3v_p} \left(\frac{q}{\mu} \right)^{1/2}. \quad (13)$$

Both spherical and cylindrical modes of agglomeration can occur in nature. The competition between these two modes is the origin of the dendritic shape that occurs throughout nature.

The constructal law requires the architecture of the agglomerate to evolve in time in such a way that the global rate of accumulation of the particles is maximized. The total current of particles ($\dot{N}_{sp} = A_{sp} \dot{n}_{sp}$) that bind to a spherical surface (area $A_{sp} = \pi D^2$) is

$$\dot{N}_{sp} = \frac{\pi K}{2v_p} D^{3/2}, \quad (14)$$

while the total current of particles that bind to a cylindrical surface (length L , area $A_{cy} = \pi dL$) is given by

$$\dot{N}_{cy} = \frac{2K}{v_p} L d^{1/2}. \quad (15)$$

While from equation (13) we see that the flux towards a planar surface depends only on surface charge density and dipole moment, equations (14) and (15) show that the particle binding rate also depends on the geometry of the agglomerate.

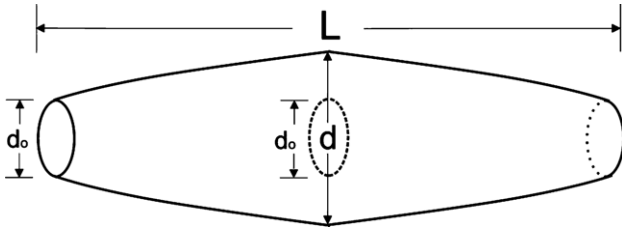


Figure 3. Needle-shaped agglomeration of particles.

For the case of a spherical agglomerate we note that $\dot{N}_{sp} = (\pi/2v_p)D^2\dot{D}$, and using equation (14) we obtain

$$D = \left(\frac{3K}{2}\right)^{2/3} t^{2/3}. \quad (16)$$

On the other hand, for a cylinder of fixed length L with $\dot{N}_{cy} = (\pi/2v_p)Ldd$, we obtain from equation (15)

$$d = \left(\frac{6K}{\pi}\right)^{2/3} t^{2/3}. \quad (17)$$

Next, we use equation (16) to calculate the volume of the spherical agglomerate

$$V_{sp} = \frac{3\pi K^2}{8} t^2. \quad (18)$$

Cylindrical growth may develop from a disc, as shown in figure 3. As the diameter increases with time (see equation (17)) the agglomerate becomes conically shaped (figure 3). In this case the growth speed along the axis is given by $\dot{L} = \dot{n}_{pl}v_p$. Then, by using equation (13) we obtain

$$\dot{L} = \frac{2K}{3} \left(\frac{q}{\mu}\right)^{1/2}. \quad (19)$$

Using equations (17) and (19) and integrating with respect to time, we find the volume of the conically shaped agglomerate:

$$V_{co} = \frac{3}{7} \left(\frac{6}{\pi}\right)^{1/3} \left(\frac{q}{\mu}\right)^{1/2} (Kt)^{7/3}. \quad (20)$$

From equations (18) and (20) we see that the ratio

$$\frac{V_{sp}}{V_{co}} = \frac{2.2}{K^{1/3}} \left(\frac{\mu}{q}\right)^{1/2} t^{-1/3} \quad (21)$$

is initially very high and that it approaches 0 as t becomes sufficiently large. According to the constructal law this means that the agglomerate must first grow as a sphere and then change to the conical shape at a critical time later in its development. From equation (21) we see that for

$$t > \frac{9.9}{K} \left(\frac{\mu}{q}\right)^{3/2} \quad (22)$$

the conically shaped agglomerate is more efficient as a particle collector than the spherically shaped agglomerate.

For water nucleating in ambient air, K is of the order of $10^{-11} \text{ m}^{3/2} \text{ s}^{-1}$ (which corresponds to a surface/water vapour field of the order of $10^{-2} \mu\text{V m}^{-1}$) and $(\mu/q)^{1/2} \sim 10^{-4} \text{ m}$. Therefore, the critical time for switching between spherical and conical growth as a preferential mode of agglomeration is

of the order of 1 s, which corresponds to $D \sim 10^{-7} \text{ m}$ as the diameter of the agglomerate. It is also interesting to compare the growth speeds of cone diameter and cone tip. By using equations (17) and (19) we obtain

$$\frac{\dot{d}}{\dot{L}} = \left(\frac{36}{K}\right)^{1/3} \left(\frac{\mu}{q}\right)^{1/2} t^{-1/3}, \quad (23)$$

which decreases as $t^{-1/3}$. This means that at later stages the agglomerate grows as a needle, the geometry of which is obtained from equations (17) and (19) (figure 3).

$$d = \left(\frac{9}{\pi}\right)^{2/3} \left(\frac{\mu}{q}\right)^{1/3} L^{2/3}. \quad (24)$$

As an example, dendritic snow crystals have a length scale of the order of 10^{-3} m , and, by taking into account equation (24), we find $d/L \sim 10^{-2} L^{-1/3}$, which for $L \sim 1 \text{ mm}$ yields $d/L \sim 10^{-2}$. This agrees with the order of magnitude of the diameter/length ratio of snowflake needles. Moreover, following equation (19) the needle tip growth speed is constant in accordance with experimental results [18].

One interesting aspect of the geometry predicted in equation (24) is that it depends only on the dipole moment μ . This means that weakly dipolar molecules will agglomerate in a needle that is more slender than the needle formed by strongly dipolar molecules.

Another noteworthy aspect is that the critical time for switching from spherical to needle-shaped growth depends only on the dipole strength, cf equation (24). From equations (16) and (22) we calculate the critical diameter of the original sphere as

$$D_{\text{crit}} \sim 6 \frac{\mu}{q} \sim 6a. \quad (25)$$

This means that a universal behaviour of particle agglomeration exists: when the sphere diameter reaches 6 particle diameters, the agglomerate (of $(\pi/6) \times 6^3 \sim 113$ particles) must switch from spherical to needle-shaped growth as a preferential mode of particle agglomeration.

Secondary needles may grow from specific points of the needle surface, generating in this way dendritic-growth architectures. A heat diffusion mechanism for explaining dendritic growth in snowflakes was proposed in [7].

In summary, the constructal law enables us to predict important features of shape generation and architecture of particle agglomeration. In the very beginning the agglomerate grows as a sphere, because at short times this shape is more effective in collecting particles from the environment.

There are many natural flow systems for which the architecture was proved to be optimized in accordance with the constructal law. Examples include the respiratory tree [19], river basins [10], bacterial growth [10], patterns of cracks on the ground [7] and dendritic crystal growth [7, 20].

3. Constructal design of air-cleaning devices

Air-cleaning devices are essential for the removal of submicrometre particles which may cause severe health problems and failure of electronic components [8, 21]. The design of air-cleaning devices is a critical aspect in new

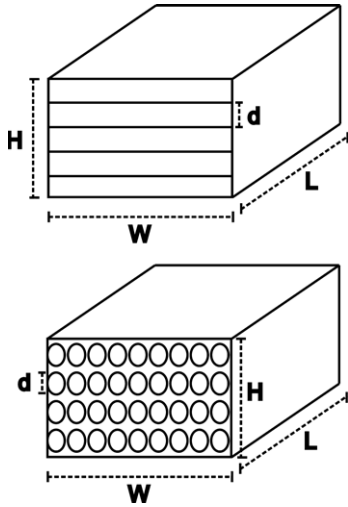


Figure 4. Schematic representation of an air-cleaning device composed of parallel-plates and tubes.

manufacturing technologies, because it impacts performance. It is also critical in the miniaturization of electronics.

Air-cleaning devices operate at low Reynolds numbers (laminar flow). Their principle of operation is this: an air stream containing particles with concentration C_{in} is forced through a set of collecting elements (e.g. plates, fibres, beds). Particles approaching the collecting elements are then transferred from the air stream to the collector surface. The challenge here is to be able to design a device with a geometry that is optimized for the capture of submicrometre aerosol. In the next two sections, we describe a constructural method for designing filter devices.

3.1. Optimal air-cleaning/sampling devices composed of tubes or channels

For simplicity, we assume that steady-state conditions prevail and that the collecting elements are smooth tubes or parallel-plates with characteristic length d (figure 4). Due to practical and economic reasons, the device must fit in a fixed volume HLW (the global constraint). The local constraint is the assumption that the aerosol particle concentration near the walls of the collecting elements must be the same as the concentration at the inlet. The global objective is for the concentration at the outlet to be the smallest possible.

Said another way, the purpose of the flow architecture is to maximize deposition rate and volumetric density. Thus, a large number of tubes/plates is required. According to figure 4, if V_{t-p} is the volume of each tube/channel and ε is the porosity of the stack, then the space allocated to the device permits the installation of $\phi (= \varepsilon WHL/V_{t-p})$ tubes/plates. While a large area available for the deposition of particles is desirable, the resulting penalty on fluid flow resistance is undesirable [2]. Therefore the optimal length d results from the competition between the number of plates for large particle deposition and increasing flow resistance. The methodology presented here is developed in two steps:

- (i) finding the limits, small- d and large- d behaviour and
- (ii) identifying the d -value that maximizes particles' deposition within the air-cleaning device.

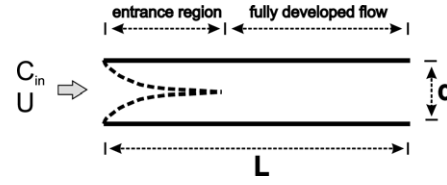


Figure 5. Boundary layers between plates with large d -spacing.

For very small d values (i.e. large ϕ), the flow is fully developed, and the outlet concentration of aerosol particles (C_o) is very small. The steady-state particle transfer rate from the air stream to the volume HLW is $HWU(C_{in} - C_o)$. The corresponding transfer density (m_p) is given by

$$m_p = \frac{HWU}{HLW}(C_{in} - C_o). \quad (26)$$

Hagen–Poiseuille flow is assumed to fill every tube/channel. The average velocity U can be related to the Poiseuille factor as [22]

$$P_0 = \frac{D_h^2}{2\eta U} \frac{\Delta p}{L}, \quad (27)$$

where D_h represents the hydraulic diameter (defined as four times the cross-sectional area of the tube or channel divided by the wetted perimeter) and P_0 is the Poiseuille factor, which is solely a function of the shape of the duct cross-section (e.g. for a round tube $P_0 = 16$ and for parallel plates $P_0 = 24$). Substituting equation (27) into equation (26) yields

$$m_p = \frac{D_h^2}{2P_0\eta} \frac{\Delta p}{L^2} (C_{in} - C_o). \quad (28)$$

For an air-cleaning device composed of tubes the hydraulic diameter is $2d$. For a device composed of parallel plates (channels) we have $D_h = 4dW/(2d + 2W)$. Because $d \ll W$, the hydraulic diameter of parallel-plates' channels is essentially $2d$. Therefore, equation (28) can be written as

$$m_p = \frac{\omega}{\eta} \frac{\Delta p}{L^2} (C_{in} - C_o) \quad (29)$$

with

$$\omega = \frac{d^2}{8} \quad (\text{tubes}) \quad (30a)$$

and

$$\omega = \frac{d^2}{12} \quad (\text{parallel plates}). \quad (30b)$$

Equation (29) shows that for very small spacings, the particle transfer density decreases in proportion to d^2 .

In the opposite limit (i.e. small ϕ), d is large enough so that each plate is coated by distinct boundary layers (figure 5). The particle transfer density to the plates is

$$m_p = \frac{\phi \lambda LZ}{HLW} (C_{in} - C_o), \quad (31)$$

where Z is the wetted perimeter. The particle transfer coefficient λ can be obtained from the Sherwood number ($Sh = \lambda L/D_{df}$) which describes the mass transfer from a flat plate into a laminar boundary layer [23]:

$$Sh = 0.664 Re_L^{1/2} Sc^{1/3} \quad (Re_L < 2 \times 10^5; 0.6 < Sc < 10), \quad (32)$$

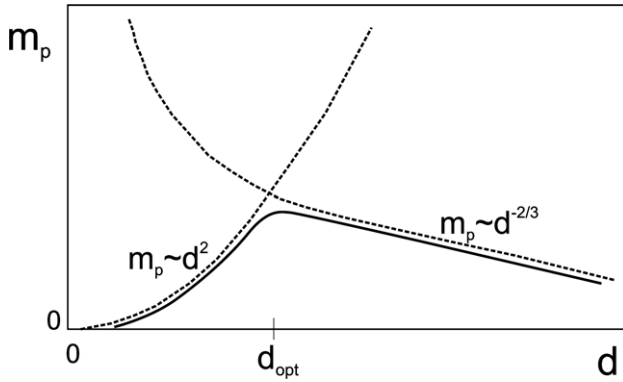


Figure 6. The intersection of asymptotes' method: optimal d -spacing.

where D_{df} is the diffusivity of particles in the air and Re and Sc are the Reynolds and Schmidt numbers, respectively. Equation (31) yields

$$m_p = 0.664 \frac{\phi D_{df} Z}{HW} \left(\frac{\rho U_o}{L\eta} \right)^{1/2} Sc^{1/3} (C_{in} - C_o). \quad (33)$$

The free-stream velocity (U_o) that sweeps the boundary layers can be obtained from the force balance on the HLW volume:

$$\Delta p HW = 2\phi\tau LW. \quad (34)$$

From laminar boundary layer theory we have

$$\tau = 0.664\rho U_o^2 Re_L^{-1/2} \quad (Re_L < 5 \times 10^5), \quad (35)$$

where the wall shear stress τ is averaged over L . Substituting equations (34) and (35) in (32) yields

$$m_p = \omega D_{df} \left(\frac{\rho \varepsilon Sc \Delta p}{\eta^2 L^4} \right)^{1/3} (C_{in} - C_o) \quad (36)$$

with

$$\omega = 1.21 H^{2/3} d^{-2/3} \quad (\text{parallel plates}) \quad (37a)$$

and

$$\omega = 1.12 \left(\frac{L^2}{W} \right)^{1/3} d^{-1/3} \quad (\text{tubes}). \quad (37b)$$

Equation (36) shows that for a device composed of tubes and parallel plates the mass rate decreases as d increases (see figure 6).

Next, we identify the d value that maximizes the rate of deposition in the air-cleaning device. The number of tubes/plates for which the particle transfer density is maximum can be determined by using the method of intersecting the asymptotes. The intersection of asymptotes method was developed as a problem solving method for convection [23]. According to this method, the intersection of two highly dissimilar trends (equations (29) and (36)) determines the spacing for the optimal internal structure. In the case of an air-cleaning device composed of parallel plates, the intersection of the two $m_p(d)$ asymptotes (figure 6) yields

$$\frac{d_{opt}}{L} \sim 2.73 \left(\frac{L^2 \Delta p}{\eta D_{df}} \right)^{-1/4}, \quad (38)$$

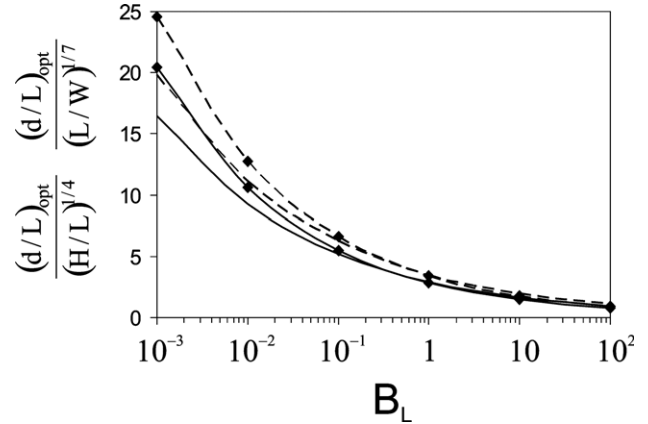


Figure 7. $(d/L)_{opt}/(H/L)^{1/4}$ and $(d/L)_{opt}/(L/W)^{1/7}$ groups versus porosity and B_L number ($\varepsilon = 0.75$: — plates —◆— tubes; $\varepsilon = 0.99$: - - - plates - - -◆- - tubes).

where $B_L = L^2 \Delta p / \eta D_{df}$ is a dimensionless group that in mass transfer plays the same role as the Bejan number proposed for forced convection heat transfer [24, 25]

$$\frac{d_{opt}}{L} \sim 2.73 B_L^{-1/4}. \quad (39)$$

Equation (39) indicates the optimal structure for maximum particle transfer to the plates that compose the air-cleaning device and also solves the problem of packing the maximum particle transfer rate into a fixed volume. The elementary construct in this optimal structure is a plate (figure 5) whose length matches the entrance length L_{opt} . The particles that are present in the core formed between boundary layers that do not merge fail to interact with the walls. On the other hand, if the boundary layers merge before the trailing edge, the particles do not interact with the walls, again because they have interacted already when they were in the boundary layers. The midrange in which the particle transfer density reaches its maximum is identified by intersecting the curves that represent equations (29) and (36). This corresponds to boundary layers that merge in the exit plane. For a device composed of parallel plates we find

$$\frac{(d/L)_{opt}}{(H/L)^{1/4}} = 3.54 \varepsilon^{2/3} B_L^{-1/4}. \quad (40)$$

In the case of an air-cleaning device composed of tubes, intersecting equations (29) and (36) yield

$$\frac{(d/L)_{opt}}{(L/W)^{1/7}} = 3.44 \varepsilon^{2/3} B_L^{-2/7}. \quad (41)$$

Equations (40) and (41) present the optimal ratio of the plate and tube, respectively.

The variation of the $(d/L)_{opt}/(H/L)^{1/4}$ and $(d/L)_{opt}/(L/W)^{1/7}$ groups with respect to porosity and B_L are plotted in figure 7. The group $(d/L)_{opt}/(L/W)^{1/7}$ (device composed of tubes) is larger than $(d/L)_{opt}/(H/L)^{1/4}$ (device composed of plates). The results shown in figure 7 demonstrate that the optimal spacing depends strongly on B_L .

Optimal spacing means maximal particle deposition in the air-cleaning devices. Equations (29), (40) and (41) lead to

$$m_{p(d/L)_{opt}} = 1.04 \eta \varepsilon^{2/3} B_L^{1/2} (\rho Sc)^{-1} \left(\frac{H}{L^5} \right)^{1/2} (C_{in} - C_o) \quad (\text{parallel plates}) \quad (42)$$

and

$$m_{p(d/L)_{\text{opt}}} = 1.47\eta\varepsilon^{2/3}B_d^{3/7}(\rho Sc)^{-1}(L^6W)^{-2/7}(C_{\text{in}} - C_o) \quad (\text{tubes}). \quad (43)$$

Equations (42) and (43) represent the maximal particle transfer rate that corresponds to the design optimized above.

3.2. Optimal filters

Another relevant situation is the optimization of filter design. Assume that the filter (porous material) has a porosity ε and contains N collector elements (i.e. fibres, beds) with a characteristic transversal dimension d . This material is mounted on a cylindrical frame of volume V . We assume steady-state laminar flow described by Darcy's law ($Re < 1$). The superficial velocity (U) is related to the intrinsic (internal) velocity (U_i) through porosity, i.e. $U_i = U/\varepsilon$.

In order to use the intersection of asymptotes method, we need to obtain the particle transfer rate in the two extremes: (i) when the collectors are very close to each other and (ii) when they are sufficiently far apart. If the collecting elements are very close to each other (i.e. in the small-porosity limit), the steady-state particles' transfer rate from the air stream to volume HLW is $AU(C_{\text{in}} - C_o)$. The corresponding particle transfer density (m_p) is

$$m_p = \frac{U}{L}(C_{\text{in}} - C_o). \quad (44)$$

Substituting Darcy's law into equation (44) we obtain

$$m_p = \frac{\kappa}{\eta} \frac{\Delta p}{L^2} (C_{\text{in}} - C_o), \quad (45)$$

where κ is permeability of the porous material. The permeability is related to the porosity ε and the characteristic length of the filter collector (e.g. fibre, bed) d_K . For materials with a porosity lower than 0.85 [8, 26]

$$\kappa = \varsigma_K \frac{\varepsilon^3}{(1 - \varepsilon)^2} d_K^2 \quad (46)$$

in which ς_K is a constant (e.g. 180 for packed beds). Consequently, equation (45) becomes

$$m_p = \frac{\varsigma_K}{\eta} \frac{\varepsilon^3}{(1 - \varepsilon)^2} \frac{d_K^2}{L^2} \Delta p (C_{\text{in}} - C_o). \quad (47)$$

In the opposite limit (large-porosity spacing, $\varepsilon \sim 1$), the intrinsic and superficial velocities are small and very similar. Therefore, diffusion becomes the predominant process, and the steady-state particle transfer rate from the air to the collector is $m_p = \varsigma_m D_{\text{df}} d_K (C_{\text{in}} - C_o)$. The total particle transfer density to the N collector becomes

$$m_p = N \varsigma_m D_{\text{df}} \frac{d_K}{V} (C_{\text{in}} - C_o), \quad (48)$$

where ς_m is a constant that depends on the collector geometry (e.g. 2π for packed beds). Because N and ε are related,

$$\varepsilon = 1 - \varsigma_\varepsilon \frac{N d_K^3}{V}. \quad (49)$$

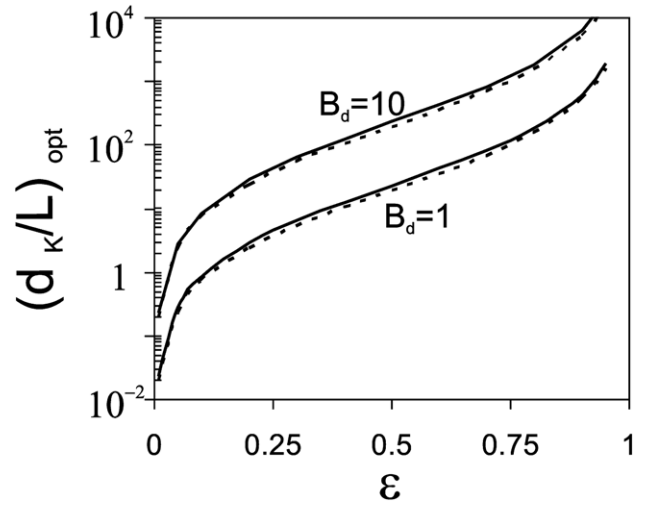


Figure 8. Optimal $(d_K/L)_{\text{opt}}$ group versus geometric arrangement and B_d number (— cubic packing; - - - hexagonal packing).

Equation (48) becomes

$$m_p = \varsigma_{m\varepsilon} (1 - \varepsilon) \frac{D_{\text{df}}}{d_K^2} (C_{\text{in}} - C_o), \quad (50)$$

where $\varsigma_{m\varepsilon}$ is a parameter that depends on the geometric arrangement (for example, $\pi/6$ for a cubic packing and $\pi/3(2)^{1/2}$ for a hexagonal packing of spheres) and $\varsigma_{m\varepsilon}$ results from the combination of ς_m with ς_ε (i.e. $\varsigma_m/\varsigma_\varepsilon$).

The particle transfer density reaches its maximum when the curve representing the number of particles transferred from the air stream to the volume V (equation (47)) meets the curve of the number of particles transferred from the air stream to N collectors available in the porous material (equation (50)). If the goal is to obtain the filter design based on collector element and thickness optimization, then from equations (47) and (50) it follows that

$$\left(\frac{d_K}{L}\right)_{\text{opt}} = \left[\frac{1}{\varsigma} \frac{\varepsilon^3}{(1 - \varepsilon)^3} B_d\right]^{1/2}. \quad (51)$$

If the purpose is porosity optimization, then

$$\varepsilon_{\text{opt}} = \left(\frac{\varsigma}{B_d} \frac{d_K}{L}\right)^{1/3} \left[1 + \left(\frac{\varsigma}{B_d} \frac{d_K}{L}\right)^{1/3}\right]^{-1}, \quad (52)$$

where ς is $\varsigma_{m\varepsilon}/\varsigma_K$ and B_d is the pressure drop number defined in terms of dimension of the collecting element ($d_K^2 \Delta p / \eta D_{\text{df}}$).

Equations (51) and (52) show the optimal geometrical groups that form such that the deposition of particles is maximum. Equation (51) defines the optimal group (d_K/L) for a specified porosity, and equation (52) defines the optimal porosity for a specified group structure (d_K/L) .

The variation of optimal $(d_K/L)_{\text{opt}}$ and ε_{opt} groups with respect to geometric parameters and B_d number is plotted in figures 8 and 9. These figures show that the effect of the packing characteristics of the filter on both optimal groups is small. The optimized architecture is strongly dependent on the pressure difference based number (B_d).

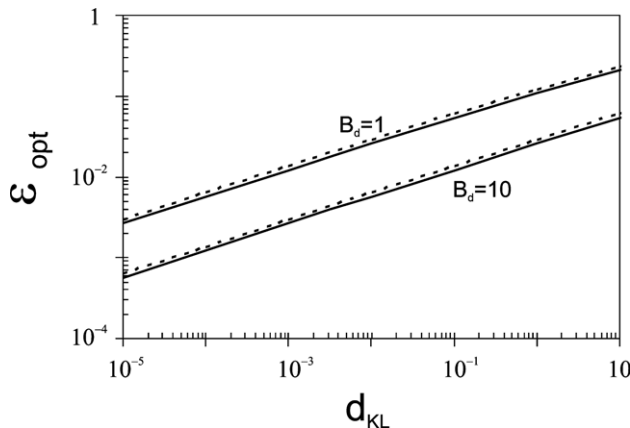


Figure 9. Optimal ε_{opt} group versus geometric arrangement and B_d number (— cubic packing; - - - - hexagonal packing).

Based on this formulation, we are also able to obtain the maximal particle transfer rate of a new type of optimized filter. From equations (47) and (52) we obtain

$$m_{\text{peopt}} = \varsigma_{\text{me}} \frac{\eta}{\rho L^2 Sc} \left(\frac{d_K}{L} \right) \left[1 + \left(\frac{\varsigma}{B_d} \frac{d_K}{L} \right)^{1/3} \right]^{-1} (C_{\text{in}} - C_o). \quad (53)$$

This equation stresses the importance of the geometric characteristics of the filter (ς , L , d_K), fluid properties (ρ , μ) and dimensionless numbers (B_d , Sc) on the maximal particle transfer rate of a brand new filter.

4. Concluding remarks

In this paper we deduced optimal features of aerosol filtration process in the framework of the constructal theory. The generation of optimal architecture for maximal global performance under global constraints in freely morphing systems is the action of constructal law [6].

In the first part of this paper we showed that the structure of particle agglomeration is generated in the pursuit of the equilibrium in the fastest way (constructal law), i.e. through the maximization of particle agglomeration rate. At small times, spherical agglomeration of particles around a particle collector is the most effective mechanism. After a critical time the configuration switches from spherical symmetry to needle-shaped agglomeration, which performs best as a particle collector at long times. Secondary needle developments give rise to dendritic patterns. It was shown that the shape of the needle depends on the dipolar moment of the particles and that the critical number of particles in the spherical agglomerate before switching to needle shape does not depend on the particle properties.

The second part of the paper used the same configuration-generation principle to design air-cleaning devices. Two geometries were considered: a device composed of parallel-plate channels or tubes and a filter. We pursued geometries that combine maximum deposition of fine aerosol particles

with low flow resistance. To achieve this goal we made sure that the fluid containing the particles and every volume element of the air-cleaning device interacted. The optimal design is the one that maximizes the transport of particles between the stream and the solid elements that form the air-cleaning device. This lead to an elemental channel/tube (d/L) and filter element (d_K/L) that is a function of geometry and pressure difference.

We also showed that the optimized shape and structure of the systems results from the trade-off between maximum collecting area and increasing flow resistance. This is the constructal design of optimal spacings [7] and the 'optimal distribution of imperfection' principle that generates the geometric form of numerous natural and man-made systems.

References

- [1] Shapiro M and Brenner H J 1990 *J. Aerosol Sci.* **21** 97
- [2] Spurny K R 1998 *Advances in Aerosol Filtration* (Washington, DC: CRC Press)
- [3] Siegel R W 1986 *Nanophase Materials: Synthesis, Structure and Properties (Series in Materials Science vol 27)* ed F E Fujita (Berlin: Springer)
- [4] Kecskes L J and Woodman R H 2003 *Scr. Mater.* **48** 1041
- [5] Kim W S and Yoon W Y 2004 *Electrochim. Acta* **50** 541
- [6] Bejan A 1997 *Advanced Engineering Thermodynamics 2nd edn* (New York: Wiley) chapter 13
- [7] Bejan A 2000 *Shape and Structure, from Engineering to Nature* (Cambridge: Cambridge University Press)
- [8] Bejan A, Dincer I, Lorente S, Miguel A F and Reis A H 2004 *Porous and Complex Flow Structures in Modern Technologies* (Berlin: Springer)
- [9] Poirier H 2003 *Sci. Vie* **1034** 44
- [10] Rosa R N, Reis A H and Miguel A F 2004 *Bejan's Constructal Theory of Shape and Structure* (Évora, Portugal: University of Évora Press)
- [11] Torre M 2004 *La Macchina del Tempo* **5** 36
- [12] Filippova O and Hänel D 1996 *J. Aerosol Sci.* **27** S627
- [13] Lehmann M J and Kasper G 2002 *Proc. Int. Workshop on Particle Loading and Kinetics of Filtration in Fibrous Filters (Institut für Mechanische Verfahrenstechnik und Mechanik, Universität Karlsruhe, Germany, 2002)*
- [14] Yang G and Biswas P 1999 *J. Colloid Interface Sci.* **211** 142
- [15] Kanaoka C 1998 *Advances in Aerosol Filtration* ed K R Spurny (Washington, DC: CRC Press) p 323
- [16] Przekop R, Moskal A and Gradon L 2003 *J. Aerosol Sci.* **34** 133
- [17] Filippova O and Hänel D 1997 *Comput. Fluids* **26** 697
- [18] Libbrecht K G 2005 *Rep. Prog. Phys.* **68** 855
- [19] Reis A H, Miguel A F and Aydin M 2004 *Med. Phys.* **31** 1135
- [20] Bejan A 1999 *Rev. Gen. Therm.* **38** 653
- [21] Wilson R and Spengler J 1996 *Particles in Our Air: Concentrations and Health Effects* (Cambridge, MA: Harvard University Press)
- [22] Mortensen N A, Okkels F and Bruus H 2005 *Phys. Rev. E* **71** 057301
- [23] Bejan A 2004 *Convection Heat Transfer 3rd edn* (New York: Wiley)
- [24] Bhattacharjee S and Grosshandler W L 1988 *ASME HTD* **96** 711
- [25] Petrescu S 1994 *Int. J. Heat Mass Transfer* **37** 1283
- [26] Pinela J, Kruz S, Miguel A F, Reis A H and Aydin M 2005 *Proc. 16th Int. Symp. on Transport Phenomena (Prague, 2005)* ed J Jezek, p 159